Contract No:

This document was prepared in conjunction with work accomplished under Contract No. DE-AC09-08SR22470 with the U.S. Department of Energy (DOE) Office of Environmental Management (EM).

Disclaimer:

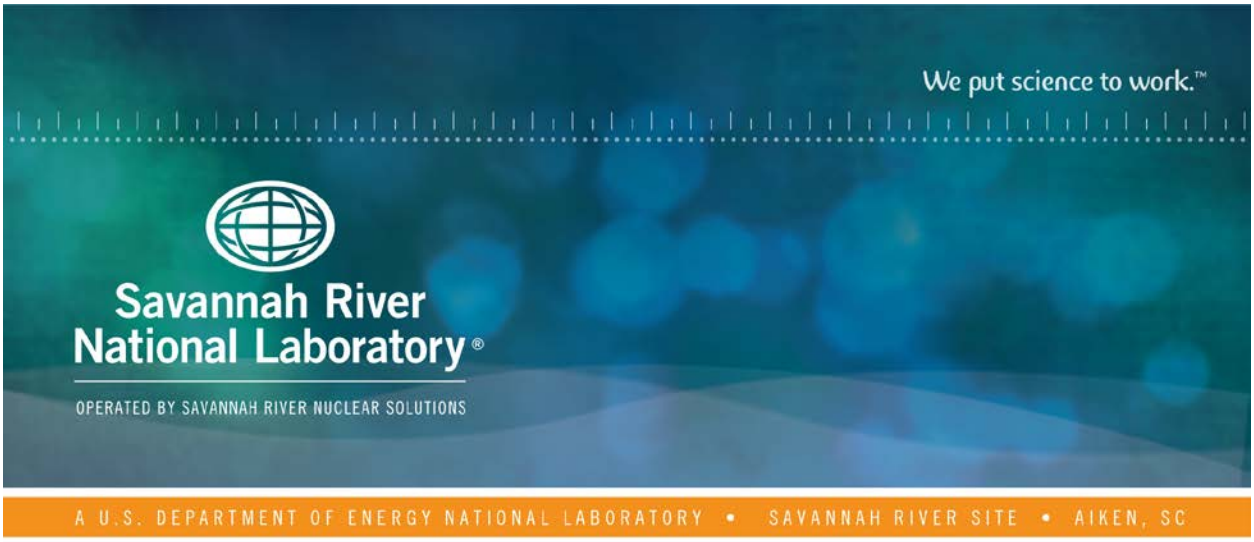

Influence of Glycolate Anion on Aqueous Corrosion in DWPF and Downstream Facilities – SCC Testing

J.I. Mickalonis

February 2020

SRNL-STI-2020-00020, Revision 0

DISCLAIMER

Printed in the United States of America

Prepared for
U.S. Department of Energy

SRNL-STI-2020-00020
Revision 0

Keywords: *glycolic acid, formic acid, DWPF, corrosion, high-nickel alloys, stainless steels*

Retention: *Permanent*

Influence of Glycolate Anion on Aqueous Corrosion in DWPF and Downstream Facilities – SCC Testing

J. I. Mickalonis

February 2020

Prepared for the U.S. Department of Energy under contract number DE-AC09-08SR22470.

Savannah River National Laboratory®
OPERATED BY SAVANNAH RIVER NUCLEAR SOLUTIONS

REVISION LOG

Revision	Sections Affected	Description of Revisions
0	All	Initial issue

REVIEWS AND APPROVALS

AUTHOR:

_____

J. I. Mickalonis, SRNL/Material Science & Engineering

TECHNICAL REVIEW:

_____

R. E. Fuentes, SRNL/Material Science & Engineering, Reviewed per E7 2.60

APPROVAL:

_____

B. J. Wiersma, Lead, Corrosion Science & Engineering
SRNL/Materials Science & Engineering/

_____

A. D. Cozzi, Manager, Applied Materials Research
SRNL/Materials Science & Engineering

_____

S. D. Fink, Manager
SRNL/ Chemical Processing Technologies

_____

J. E. Occhipinti, Manager
SRR/Tank Farm Facility Engineering

_____

T. H. Huff, Manager
SRR/Defense Waste Processing Facility & Saltstone Facility Engineering

ACKNOWLEDGEMENTS

The author wishes to acknowledge the following individuals for their assistance with the experimental work and project management as well as helpful technical discussions:

B. T. Hill
T. H. Murphy
D. M. Missimer
B. J. Wiersma
R. E. Fuentes

EXECUTIVE SUMMARY

Glycolic acid is being evaluated as an alternate reductant in the preparation of High Level Waste for the Defense Waste Processing Facility (DWPF) at the Savannah River Site (SRS). During processing, the glycolic acid may not be completely consumed with small quantities of the glycolate anion being carried forward to waste facilities. The SRS liquid waste contractor requested an assessment of the influence of the glycolate anion on the corrosion of the materials of construction (MoC) throughout the waste processing system since this concern had not been previously evaluated. The influence of glycolic acid on the occurrence of stress corrosion cracking (SCC) had not been evaluated specifically in the previous testing. The present testing used electrochemical and coupon immersion testing to assess this influence. Additionally, the primary guidance on corrosion for operating DWPF with a formate-based flowsheet is based on testing that utilized test solutions with a small number of constituents. Recent testing used more complex solutions based on flowsheet development for DWPF. Additional electrochemical tests were also conducted to assess the influence of this difference on test results.

The results from both the electrochemical and coupon immersion tests in formate-based and glycolate-based solutions with chlorides concentrations between 800 and 1200 parts per million showed no active forms of localized corrosion. The Cyclic Potentiodynamic Polarization (CPP) scans in these solutions had passive regions with some degree of positive hysteresis which indicate a possibility for the occurrence of localized corrosion. The positive hysteresis occurred at potentials greater than 200 mV more electropositive than the corrosion potential indicating that, at least, crevice corrosion should not occur in service. The three-month coupon immersion tests, however, showed no form of localized corrosion (SCC, crevice corrosion and pitting) occurred under simulated operating conditions. The coupon immersion test also showed that deposits are likely to form on C276 during service especially near the vapor/liquid interface.

The CPP testing also showed that some differences occur with using five-constituent DWPF simulants (i.e. simple) as opposed to the more complex multi-constituent solution chemistry used in this testing. The testing was performed to establish a comparison point between older corrosion data (1980-90's) obtained with simple solution chemistry and the newer data. Tests with glycolate-based solutions, which were not tested prior to this study, the CPP data did not show a significant difference in corrosion behavior. For formate-based solutions, the difference was more significant with a change in operable corrosion mechanisms (i.e., anodic corrosion for a simple chemistry versus passivity for a complex chemistry). However, the lack of susceptibility to localized corrosion was found to be the same.

TABLE OF CONTENTS

LIST OF TABLES

LIST OF FIGURES

LIST OF ABBREVIATIONS AND SYMBOLS

ASTM	American Society for Testing and Materials International
CPC	Chemical Processing Cell
CPP	Cyclic Potentiodynamic Polarization
CR	Corrosion Rate
DWPF	Defense Waste Processing Facility
E_b	Breakdown Potential (V, SCE)
E_{corr}	Corrosion Potential (V, SCE)
E_{rp}	Pit Repassivation Potential (V, SCE)
EW	Equivalent Weight
i_{pass}	Passive current density (A/cm^2)
LPR	Linear Polarization Resistance
MoC	Material of Construction
mpy	Mils per year
ND	No Data
OCP	Open Circuit Potential
ppm	parts per million
R_p	Polarization Resistance
SA	Surface Area
SCC	Stress Corrosion Cracking
SCE	Saturated Calomel Electrode
SIP	Structural Integrity Program
SRNL	Savannah River National Laboratory
SRS	Savannah River Site
WAC	Waste Acceptance Criteria

1.0 Introduction

The Savannah River Site (SRS) is preparing for an alternate reductant flowsheet for the Defense Waste Processing Facility (DWPF), specifically a nitric acid-glycolic acid flowsheet. DWPF requested a corrosion assessment from the Savannah River National Laboratory (SRNL) for the components of the DWPF facility and the other High Level Waste and Low Level Waste processing facilities that would be exposed to glycolic acid or the glycolate anion [1]. Testing was conducted in both aqueous and glass environments [2]. Follow on testing was required to further investigate several issues for aqueous environments: 1) several results where localized corrosion was observed on test samples; 2) the influence of glycolic acid for all the different waste compositions covered by the Tank Farm Corrosion Control Program; and 3) a new chloride corrosion limit for the DWPF Waste Acceptance Criteria (WAC), which was established at 800 ppm [3, 4]. Testing was also recently completed for verifying that the Recycle Collection Tank, waste transfer line, and waste tank materials of construction (MoC) did not experience aggravated corrosion from the use of permanganate in that tank for glycolate destruction [5]. Additional follow-up testing for the melter refractory material was also conducted and is covered in a separate report [6].

The DWPF vessels are protected in part by the Structural Integrity Program (SIP), which is based on early material research for the DWPF as well as the coupon and vessel assessments performed after nonradioactive commissioning [7]. The SIP assesses numerous forms of corrosion including general, pitting, crevice, galvanic, intergranular and stress corrosion cracking (SCC). SCC was not considered to be a viable corrosion mechanism and had not previously been included in the assessment of the influence of glycolic acid. Since C276 appeared to have a chloride sensitivity in DWPF simulants at the boiling condition (i.e., within the Chemical Process Cell (CPC)), verification of SCC resistance for C276 was determined to be necessary for the presence of derivatives of both reductants, glycolic acid and formic acid [8, 9]. SCC is not known to have caused a catastrophic or any known failure within the CPC, so formate-bearing test solutions are expected to show a null result.

Much of the early DWPF material testing was performed in solutions using three to five constituents (i.e., simple), while the recent glycolic acid material testing used solutions with multiple constituents (i.e., complex) which formed precipitates. The new WAC limits were established from testing with the precipitates present in the test solutions. These complex solutions more closely resemble DWPF sludges. The presence of deposits on test coupons was a contributor to the observed corrosion and occurred in part from the presence of the precipitates in solution. For the SCC susceptibility testing, electrochemical testing was recommended to evaluate the influence of differences in solution chemistry (i.e., simple and complex) on corrosion susceptibility for C276 [9].

This testing for C276 SCC susceptibility consisted of accelerated electrochemical corrosion testing and a three-month coupon exposure test. The electrochemical testing provided broad data on the potential for SCC susceptibility. Data was also obtained about the complexity of solution chemistry and if the WAC chloride corrosion limit of 800 ppm is close to a concentration where localized corrosion resistance is notably reduced (i.e., 1000 and 1200 ppm Cl). The 3-month coupon exposure test was performed with welded teardrop-shaped and creviced coupons totally immersed and at the liquid/vapor interface. This type of testing is similar to the use of twisted coupons used during the initial DWPF materials testing [10]. The results of these tests are reported here-in and this approved report meets deliverable #3 of HLW-DWPF-TTR-2013-0004 [1].

2.0 Experimental Procedure

The testing for C276 SCC susceptibility in glycolate and formate-bearing solutions consisted of two test types: electrochemical, which included a series of accelerated techniques, and coupon immersion. The test techniques/protocols, solutions, and materials used for these tests are discussed.

2.1 Electrochemical Testing

The electrochemical testing was chosen as an accelerated method to determine if the glycolic acid would influence the localized corrosion resistance of the MoCs as well as to measure a general corrosion rate. The electrochemical testing followed the guidelines given in applicable American Society for Testing and Materials (ASTM) International standards [11-15]. The electrochemical testing consisted of a series of individual tests including open-circuit potential (OCP) measurement, linear polarization resistance (LPR) and cyclic potentiodynamic polarization (CPP).

OCP monitoring was used to follow the equilibration of the sample in the test solution and varied from one hour up to of three hours. Immediately at the end of the OCP monitoring, LPR was performed to determine a general corrosion rate. This test involves application of a scanning potential ramp (0.2 mV/sec) over a potential range of +/- 15 mV around the OCP. From the plot of the potential and resulting current, a polarization resistance value (R_p) is determined and Equation 1 is used to calculate a general corrosion rate (CR) for the material in mils per year (mpy).

$$CR = 3.27\ 10^3 \times B \times EW / (R_p \times \rho \times SA) \qquad \{Equation\ 1\}$$

where B[1] is a constant related to the electrochemical behavior of the material in the environment, 0.026 for this testing; EW is the equivalent weight of the material (dimensionless); ρ is the material density (g/cm^3); and SA is the surface area of the sample (cm^2). For C276, the material applicable values for Equation 1 are as follows: density – 8.8 g/cm^3, and equivalent weight – 27.09. The nominal coupon surface area was 4.5 cm^2

At the conclusion of the LPR, a CPP was performed to assess the susceptibility to localized corrosion. In this technique, a potential ramp (0.2 mV/sec) is applied towards more electropositive potentials reaching a defined vertex (maximum potential or current limit) where the potential scan direction is reversed back towards the OCP. In this testing, the current limit (1 mA/cm^2) was reached during the scan prior to the inputted maximum potential. The potential/responding current plot provides data on the passivity and susceptibility to pitting, crevice corrosion and SCC. An indication of pitting susceptibility is determined by the hysteresis which occurs between the reverse and forward scans.

Schematic CPP curves are shown in Figure 2-1 highlighting the key parameters measured from the curves and the different type hystereses observed in the curves for determining localized corrosion susceptibility. An indication of pitting susceptibility is a positive hysteresis which occurs when the reverse trace (dotted line) is at larger currents than those of the forward trace (solid line) as shown in Figure 2-1C. A negative hysteresis, shown in Figure 2-1A, occurs when the reverse trace is at lower current than the forward trace and generally, indicates a material is not susceptible to pitting or crevice corrosion.

In many cases, a reverse trace starts with a larger current than the forward trace but with decreasing potentials the current difference decreases until the reverse trace crosses the forward trace. The potential where this crossover occurs is identified as the pit protection potential or the pit repassivation potential (E_{rp}) as shown in Figure 2-1B. The E_{rp} identifies a potential below which the material is immune from the continued propagation of any pit that formed. At potentials greater than $E_{rp,}$ a pit may grow. A pit initiates when the potential exceeds a given breakdown potential, E_b. E_b could either be a pit initiation potential or the start of the transpassive region where the conditions are highly oxidizing and the material surface oxides

[1] B was calculated using anodic and cathodic Tafel slopes of 0.12 V/decade [7, 9] as a comparative value for all MoCs. For these passive or corrosion resistant alloys, general corrosion was not of primary concern. The general corrosion rate values were only used to determine if a significant change occurred with chemistry and not used to calculate an accurate rate. These rates are considered to be conservative since passive materials have lower Tafel slopes.

are less corrosion resistant, and more susceptible to localized corrosion, including intergranular attack and stress corrosion cracking.

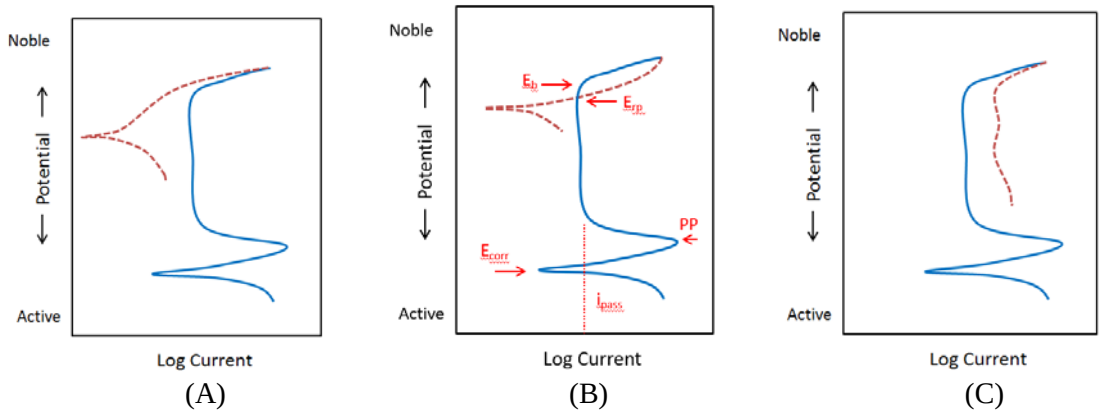

Figure 2-1. Schematic CPP curves (blue curve is forward trace; red curve is reverse trace) showing key parameters: A) negative hysteresis; B) positive hysteresis with Erp; and C) positive hysteresis

Other parameters measured from the CPP scans include a corrosion potential, E_{corr}, and a passive current density, i_{pass}. The value of E_{corr} and OCP are generally close in value and a quasi-steady state potential where the anodic and cathodic currents on the surface are balanced. For passive metals such as C276, a potential (the passivation potential, PP in Figure 2-1B) is reached where the current (i_{pass}) is independent of potential due to the presence of a corrosion resistant oxide. The current density that can pass through the oxide is called the passive current density and is a measure of the material corrosion resistance.

Although E_{rp} may be identified during testing, pitting during service depends if the same specific conditions (i.e., temperature, local surface chemistry, etc.) may exist in the field since oxidizing conditions are necessary. The natural potential of the material in the environment is the OCP or E_{corr} which is measured from the CPP curve. If E_b and E_{rp} occur at highly oxidizing conditions, i.e. significantly more positive than OCP or E_{corr}, this condition may not be established during normal service. The potential difference, $E_{rp} - E_{corr}$, is a corrosion industry value used to indicate if pitting would be expected. A value greater than 100-200 mV indicates pitting would not be expected [16].

The electrochemical tests were performed with Gamry Reference 600 potentiostats which was software controlled with a laptop computer for data acquisition. The potentiostat performance was verified following the test guidelines given in ASTM International G5 standard reference test method [6]. The test cell consisted of borosilicate glass five-port flasks with a standard three-electrode set up: counter, reference and working electrodes. The counter electrode was two 0.25-inch diameter graphite rods connected with a wire, while the reference electrode was a saturated calomel electrode (SCE, +0.243 V vs Normal Hydrogen Electrode). All potentials in this report are given in reference to the SCE potential. Prior to each test, the reference electrode potential was verified against that of an unused reference maintained in a saturated potassium chloride solution. After the potential check, the reference electrode was placed in a salt bridge containing 0.1 M sodium nitrate solution for performing the tests.

The working electrodes were C276 bullets (3.2 cm length by 0.47 cm OD, SA – ~4.5 cm^2) obtained from Metal Samples, Inc. (Munsford AL). The surface was prepared with 600-grit silicon carbide paper prior to testing. After the test, the samples were examined for corrosion. The nominal composition (wt%) of C276 is 15.5 Cr, 57.8 Ni, 6.3 Mo, 0.5 Mn, 14.2 Fe, 0.3 Si, 3.3 W, and 1.8 Co.

Test solutions were prepared up to one day prior to performing the test. Batch size was 1.2L so duplicate tests were performed from each batch (600 mL in each test vessel). After testing, deposits or precipitates were seen in the bottom of the test cell. Measurement of the solution pH was made before and after each test. Tests were performed without bubbling air. Testing was performed at temperatures between 95-98 °C using a digital hotplate. The natural convection of solutions due to heating from the bottom provided for some solution mixing.

In this testing, two chloride concentrations higher than the new WAC corrosion limit of 800 ppm were evaluated (see Section 2.3 for a more complete description of test solutions). 1000 ppm was tested for both reductants. With favorable results at 1000 ppm, a concentration of 1200 ppm was tested. The higher values will confirm that the WAC limit is not near a concentration of increased susceptibility. The CPP scans obtained from this testing were compared with those obtained previously for developing the new chloride concentration WAC corrosion limit to assess any change in localized corrosion susceptibility.

2.2 Coupon Immersion Tests

Laboratory coupon immersion tests are used to assess the corrosion performance of materials and to understand the influencing factors under controlled, simulated industrial environments. The SRNL coupon immersion testing followed the guidelines given in ASTM International G31 standard practice [15]. The coupon immersion tests were performed to evaluate the corrosion in the CPC vessels over an extended period (3 months) with simulated CPC supernates and typical operating temperatures (i.e., boiling). The tests were conducted in borosilicate glass containers using laboratory digital hot-plates for temperature control as shown in Figure 2-2(A). Each container had a condenser that was connected to a chilled water circulator to minimize evaporative losses. The test solutions were based on the results from the electrochemical testing. For each reductant, chloride concentrations were 800 and 1200 ppm (see Section 2.3 for a more complete description of test solutions).

(A) **(B)**

Figure 2-2. Coupon immersion test: (A) setup of four vessels; (B) close up of hanging coupons

Three different coupons were used in the coupon immersion test; specifically a tear-drop shaped coupon (10 cm×1.95 cm×0.15 cm) for testing C276 in a stressed condition, a flat rectangular coupon (5.1 cm×2.5 cm×0.3 cm) for determining a general corrosion rate, and a flat rectangular coupon (5.1 cm×1.95 cm×0.3 cm) with a central hole for attaching of a ceramic crevice assembly. Coupons were exposed on a borosilicate support that was hung from the container lid as shown in Figure 2-2(B). Coupons remained exposed in the solutions for the full three months. Afterwards, the coupons were rinsed with distilled water

and dried. Pictures were taken prior to and after cleaning. Coupons were cleaned in 1M nitric acid solution, thoroughly rinsed with distilled water, rinsed with ethyl alcohol and blown dry. Coupons were weighed before and after testing to calculate corrosion rates using weight loss.

2.3 Test Solutions

The solutions used in this testing were like those used in previous testing [2, 3]. The formate- and glycolate-based solutions were formulated from CPC simulants determined during flowsheet development testing to support processing of Sludge Batch #8 waste and Sludge Batch #7 waste, respectively. The solution recipes were based on chemical analysis of the experimental CPC simulants made with acid stoichiometry of 110 wt% and 140 wt% for Sludge Batches #7 and #8, respectively. The solution chemistry is shown in Table 2-1 for 800 ppm Cl. In this testing, the chloride concentration was tested at two values - 1000, and 1200 ppm. The quantity of sodium sulfate shown in Table 2-1 corresponds to 4200 ppm sulfate, the current WAC corrosion limit for sulfate. The mercury concentration was approximately 300 ppm, based on the first phase testing where this concentration was the maximum soluble concentration obtained.

Table 2-1. Composition of Glycolate- and Formate-based Complex Solutions with 800 ppm Cl

Solution Type →		**Glycolate[1]**	**Formate[1]**
Chemical	**Formula Mass (g)**	**(g/L)**	**(g/L)**
Sodium Oxalate ($Na_2C_2O_4$)	134	5.7851	5.7851
Mercury Nitrate ($Hg(NO_3)_2 \cdot H_2O$	342.62	0.5118	0.5118
Manganese Nitrate (50 wt% $Mn(NO_3)_2$ + 5 wt% HNO_3)	178.95	17.3892	19.8584
Ruthenium Chloride ($RuCl_3$) – 41.74 wt% Ru	242.14	0.0217	0
Rhodium Nitrate ($Rh(NO_3)_3$ 4.933 wt% Solution)	2086.06	0.5285	0.1867
Zirconium Nitrate ($ZrO(NO_3)_2 \cdot 6H_2O$)	339.32	0.084	0.084
Sodium Sulfate (Na_2SO_4)	142.04	6.2105	6.2105
Sodium Chloride (NaCl)[2]	58.44	1.3185	1.3185
Aluminum Nitrate ($Al(NO_3)_3 \cdot 9H_2O$)	375.13	3.01	3.01
Sodium Nitrate ($NaNO_3$)	84.99	63.6692	44.613
Magnesium Nitrate ($Mg(NO_3)_2 \cdot 6H_2O$)	256.41	2.1416	2.1416
Iron Nitrate ($Fe(NO_3)_3 \cdot 9H_2O$)	404	0.404	1.0164
Nickel Nitrate ($Ni(NO_3)_2 \cdot 6H_2O$)	290.81	0.4955	0.4955
Potassium Nitrate (KNO_3)	101.11	0.8288	0.8288
Calcium Nitrate ($Ca(NO_3)_2 \cdot 4H_2O$)	236.15	0.6423	0.6423

1. Glycolate was added as sodium salt at 63.4888 g/L and formate was added as sodium salt at 85.2027 g/L.
2. This quantity of sodium chloride is equivalent to 800 ppm. For 1000 and 1200 ppm chloride, the quantity of sodium chloride used was 1.6481 and 1.9978 g/L, respectively.

The simple solution chemistry contained only five chemicals; sodium salts of chloride, sulfate, nitrate, and glycolate or formate along with mercuric nitrate. The concentrations of the chemical species were similar to those analyzed in flowsheet CPC simulants, which were corrosion tested previously [3]. Both the glycolate- and formate-based CPC simulants caused surface deposits and crevice corrosion. These

simulants were chosen for a simple chemistry test because of the resulting corrosion previously observed so the impact of a simple chemistry on corrosion could be evaluated. The quantities of added salts are shown in Table 2-2. Gray precipitates formed during testing and were attributed to mercuric salts dropping out of solution. As can be seen by a comparison of Table 2-1 and Table 2-2, the chloride and sulfate concentrations had large differences in some cases from the new WAC corrosion limits (chloride – 800 ppm, sulfate – 4600 ppm).

Table 2-2 Composition of Glycolate-based and Formate-based Simple Solutions

Solution Type →		**Glycolate[1]**		**Formate[1]**	
Chemical	**Formula Mass (g)**	**(g/L)**	**(ppm)**	**(g/L)**	**(ppm)**
Mercury Nitrate ($Hg(NO_3)_2 \cdot H_2O$	342.62	0.5124	Hg - 300	0.5124	Hg - 300
Sodium Sulfate (Na_2SO_4)	142.04	3.8963	SO_4 - 2635	3.7719	SO_4 - 2550
Sodium Chloride (NaCl)	58.44	1.4409	Cl - 874	0.4073	Cl - 247
Sodium Nitrate ($NaNO_3$)	84.99	127.0707	NO_3 - 92700	37.7016	NO_3 - 27500

1. Glycolate was added as sodium salt at 82.2276 g/L (62950 ppm) and formate was added as sodium salt at 113.6356 g/L (75200 ppm).

During makeup of the test solutions, the chemicals were added in the order shown in Table 2-1 and Table 2-2, which was in order of increasing solubility to decrease the quantity of precipitates or sludge produced during the first set of tests. Certain chemicals still were difficult to dissolve in the complex solution, including sodium oxalate and aluminum nitrate. Solutions were generally made the day before use, placed in storage bottles, and stirred overnight. Precipitate quantity in the solution did not appear to change overnight.

Solution pH differed for the two reductant test solution types; glycolate-based solutions ranged 5-6 and formate-based solutions ranged 6-7. Small changes in solution pH (~0.2) were generally seen from testing. Three glycolate-based solutions, which had initial pH between 6.2 and 7.2, were adjusted dropwise with a nitric acid solution to approximately 5 to be consistent with other solutions.

As observed previously, the solutions underwent color changes and precipitation with heating, changing from yellow to brown or gray with white precipitates forming initially and only dark precipitates by test end. Solution analysis was not performed to characterize these changes, although final solution chemistries were obtained after testing. These analytical results for soluble elements and species are shown in Appendix A for test solutions used in the coupon immersion tests. The glycolate-based solutions were able to maintain more elements in solutions such as Fe, Ni, and Mn. Neither glycolate- or formate-based solutions were able to maintain Hg in boiling solutions, which has been noted in previous testing [2, 3].

3.0 Results and Discussion

The experimental work during this testing applied to DWPF CPC vessels and components and was focused on SCC with some additional investigation of crevice corrosion. The testing included electrochemical and coupon immersion testing, which are discussed in Sections 3.1 and 3.2.

3.1 Electrochemical Test Results

Electrochemical tests were performed to better understand if localized corrosion of C276 in both glycolate- and formate-based solutions would occur at higher concentrations than the new WAC chloride corrosion limit of 800 ppm and to assess if SCC or crevice corrosion posed any significant risk to the CPC vessels and heated components. These data were used to establish the test compositions for the three-month coupon

immersion test, discussed in Section 3.2. Additionally, tests were performed in a simple chemistry solution at 1000 ppm Cl to determine if electrochemical results differ from the complex chemistry solution used for most of the testing on the influence of glycolate on DWPF MoCs. A simple chemistry solution was used previously for material selection in the DWPF.

The electrochemical data under the current testing were obtained with 1000 and 1200 ppm Cl in both glycolate- and formate-based solutions. For the 1000 ppm Cl solutions, a simple and complex chemistry was used as described previously. These data are compared to the WAC testing data for the 800 ppm Cl solutions reported previously [3]. Some of the data differences between the 800 ppm Cl from previous testing and the current set may be due to the different bottles/sources of the starting chemicals that were used in preparing each of the test solutions.

The CPP data for C276 in glycolate- and formate-based solutions differed. Previously in formate-based solutions, the CPP data variations were attributed to a change in chloride and sulfate concentrations in the solutions, whereas for glycolate-based solutions these data were similar for the ranges of chloride and sulfate concentrations tested [3]. In the current testing, no correlation was found between the chloride concentration and the CPP data for either reductant. The results for each type of solution are presented separately below.

3.1.1 Glycolate-based Solutions

In glycolate-based solutions, the CPP scans for C276 were similar as shown in Figure 3-1. All the CPP scans had a passivation peak at about 0.2 V, a breakdown potential, E_b, near 0.45 V, and a repassivation peak, E_{rp} ranging between 0.35-0.39 V, slightly more electronegative than E_b. These values are summarized in Table 3-1 for each chloride concentration in the glycolate-based solutions along with E_{corr}, i_{pass} and CR, given in mpy. A positive hysteresis loop may indicate some localized corrosion susceptibility including SCC. In the previous testing, the positive hysteresis loop was found not to be associated with pitting [3]. The test coupons were found not to have pitted during the test and only had a slightly oxidized surface, which was similar to the pre-test morphology.

Table 3-1. Electrochemical Results for C276 in Glycolate-based Solutions as a Function of Chloride Concentration and Solution Chemistry[β]

Chloride Concentration (ppm)	Chemistry	Average Electrochemical Data					
		CR (mpy)	E_{corr} (V)	i_{pass} ($\mu A/cm^2$)	E_b (V)	E_{rp} (V)	E_{rp} -E_{corr} (V)
1000	Simple	3.58	0.090	9.6	0.431	0.390	0.300
1000	Complex	1.53	0.082	3.4	0.456	0.355	0.273
1200	Complex	1.34	0.102	3.4	0.442	0.348	0.246
800	Complex	0.05	-0.023	2.1	0.424	0.330	0.356

B. The 800 ppm Cl data was from previous testing [3].

The 1000 ppm Cl simple chemistry solution was performed to determine if initial testing performed in the 1980s using simple chemistry solutions generates similar data to the complex chemistry solutions that were used in most of the testing to assess the influence of glycolate. CPP scans were similar as shown by the data in Figure 3-1 (compare the yellow/orange and red curves) with both showing a passivation peak and positive hysteresis indicating that similar corrosion behavior should be detected. The simple chemistry CPP scan, however, had a smaller hysteresis loop as well as a smaller passive region and the corrosion rate and i_{pass} values were higher. Therefore, these simple chemistry solutions appear to be more corrosive, which may be associated with a lack of oxidizing species that lead to development of a more protective oxide on C276.

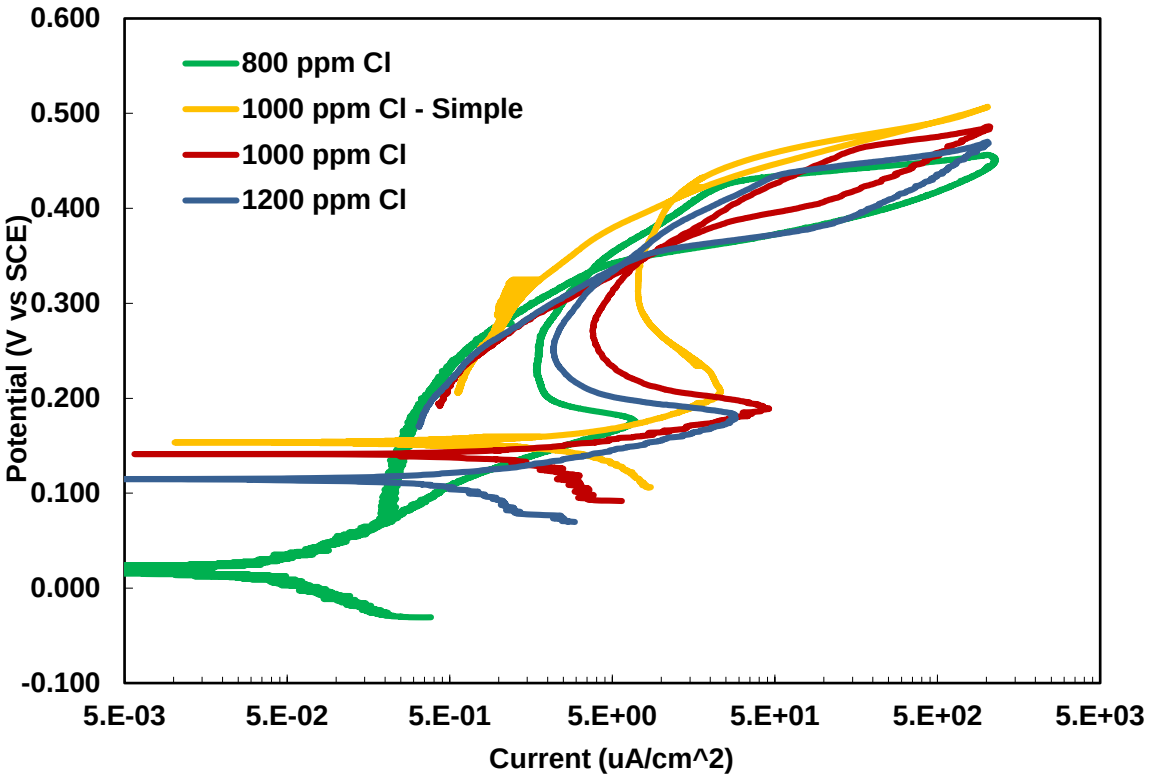

Figure 3-1. CPP scans of C276 in glycolate-based solutions with a range of chloride concentrations (800 ppm ≤[Cl^-]≤ 1200 ppm) at 95 °C; [SO_4^{-2}]=4200 ppm

As can be seen by the data in Table 3-1 and the CPP scans in Figure 3-1, the E_{corr} value for the 800 ppm Cl data is at more electronegative potentials than the remaining data that was obtained in the recent testing. These more electronegative values are believed to be a function of solution chemistry. Previously, the concentration of soluble mercury was found to influence both E_{corr} and the measured corrosion rate [2]. A higher soluble mercury concentration results in more electropositive E_{corr} and higher corrosion rates, which can be seen in the data in Table 3-1. The concentration of other oxidizing species may also influence these variables. Shifts in E_{corr} were observed in this testing for the 1000 ppm Cl test as shown in Figure 3-2 for the duplicate test performed (CPG1-1 and CPG1-2). The soluble mercury concentration for CPG1-2 might be higher than that for CPG1-1 since E_{corr}.for CPG1-2 at 0.141 V is more electropositive than E_{corr} for CPG1-1 at 0.001 V.

The CRs measured in this recent testing for the 1000- and 1200-ppm Cl solutions were greater than those measured for the WAC testing, which the 800-ppm data in Table 3-1 are representative. The higher chloride for the current testing is a contributor, along with the final soluble solution chemistry after makeup caused by variable precipitation. While these rates are greater than the 1 mpy limit specified in the DWPF SIP [7], they are only slightly greater. Additionally, the coupon immersion test provides a better measure if general corrosion is an issue since the CR calculated for the weight loss data is time averaged and is impacted by the growth of oxides over time. Electrochemical CR values are instantaneous measures which for this testing were measured after only three hours of exposure. All the test bullets were found not to have corrosion and appeared similar to an untested coupon as was observed for the WAC testing [3].

The potential difference between E_{corr} and E_{rp} provides a measure of the likelihood for occurrence of localized corrosion expected in service [16]. As can be seen by the data in Table 3-1 for these glycolic-

based solutions, E_{rp} >> E_{corr} or E_{rp}-E_{corr} > 200 mV over the range of 800-1200 ppm Cl. Even if pitting had occurred to some degree during the testing, pitting in service would not be expected.

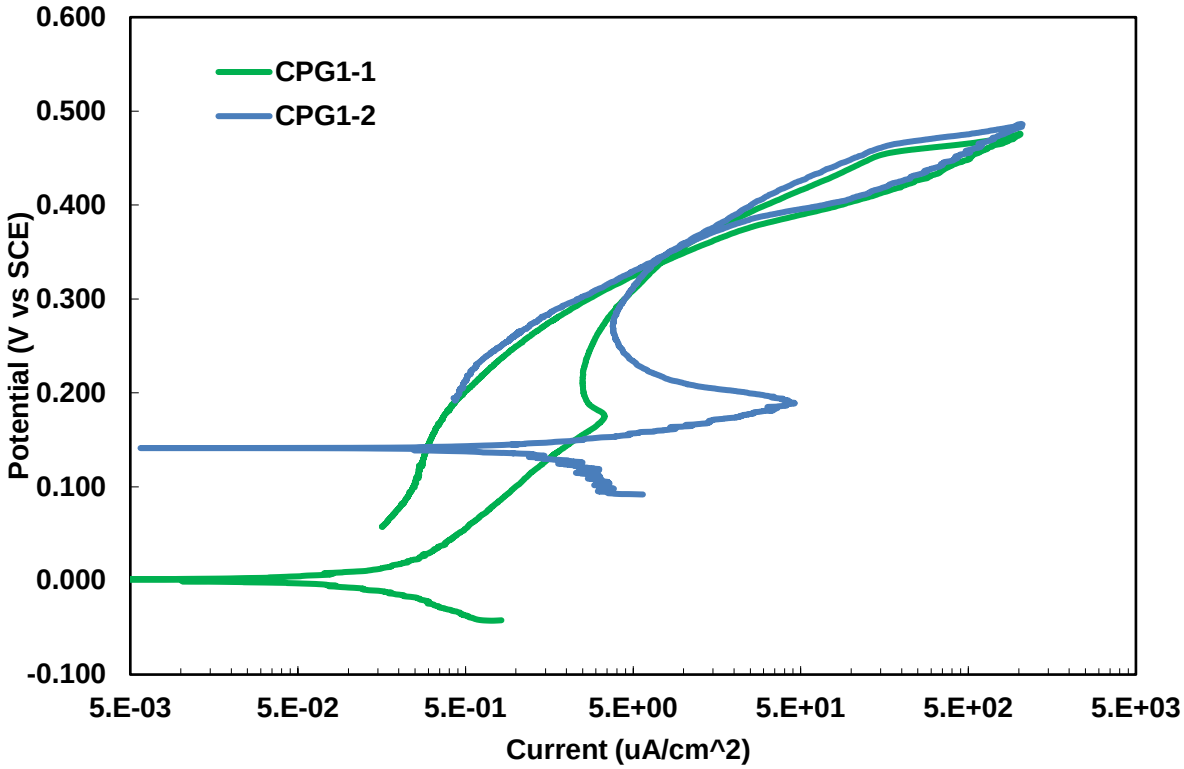

Figure 3-2. CPP scans of C276 in glycolate-based solutions at 1000 ppm Cl and 95 °C

Areas on the CPP scans for glycolate-based solutions that may indicate a SCC susceptibility include the presence of the passivation peak at approximately 0.2 V and the presence of the positive hysteresis loop. These areas are where large changes in current are observed for small potential changes and have changes in oxide structure occurring, providing an instability for SCC initiation. While the CPP scans indicate the electrochemical activity possible for C276, the actual exposure conditions may not drive the sample to these conditions. The coupon immersion test of simulated exposure without accelerating parameters, such as applied potentials, provides a more representative condition for SCC occurrence for the DWPF operating environment.

3.1.2 Formate-based Solutions

In the formate-based solution, the CPP scans for C276 were all similar for the complex chemistry solutions, as shown by the data presented in Figure 3-3, and were not a function of chloride concentration. The CPP scans showed a possible passivation region of similar size with a positive hysteresis. While the passivation region in glycolate-based solutions showed a distinctive passivation peak, such a peak was not definitively shown in formate-based solutions. The passivation region is defined by the potential range where current, i_{pass}, is independent of the potential. For these formate-based solutions, this passivation region occurred between -0.075 and 0.4 V with i_{pass} of 100 µA/cm^2. Key electrochemical parameters measured from the CPP scans are given in Table 3-2 for each chloride concentration.

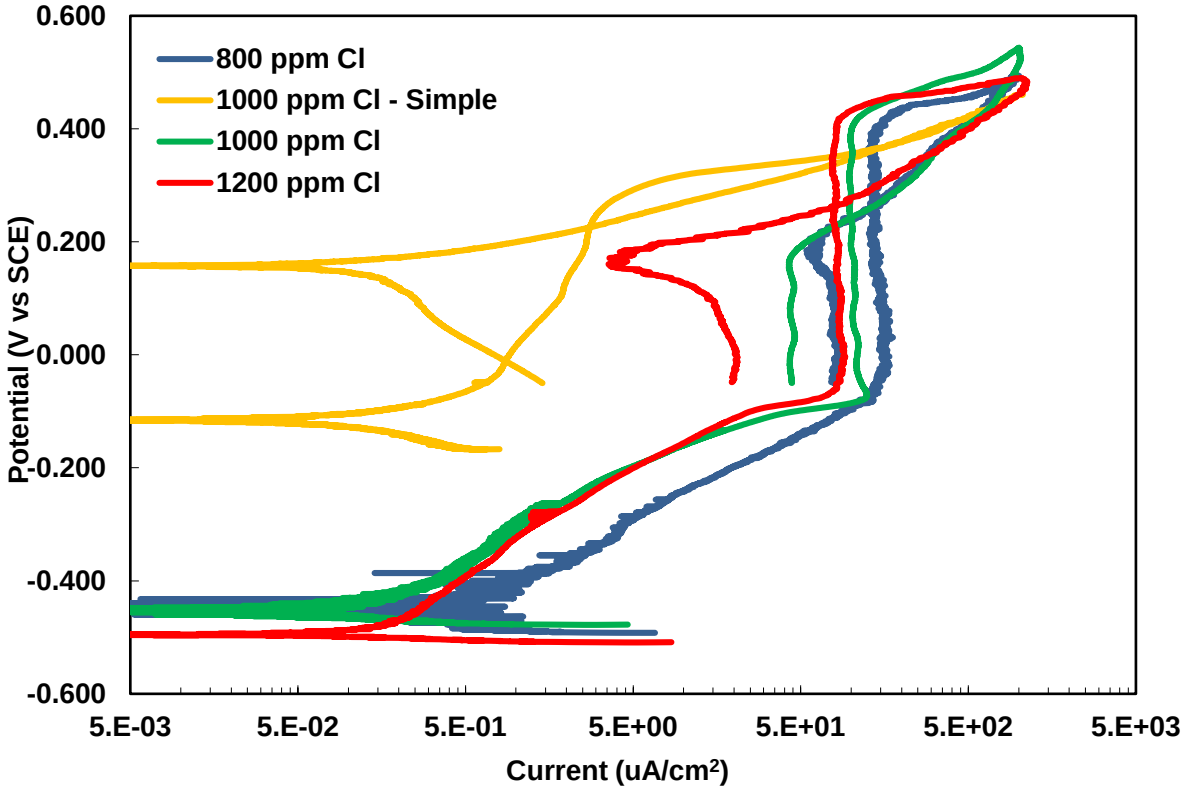

Figure 3-3. CPP scans of C276 in formate-based solutions with a range of chloride concentrations (800 ppm ≤[Cl^-]≤ 1200 ppm) at 95 °C; [SO_4^{-2}]=4200 ppm (scans have been truncated on the reverse scan for clarity)

Table 3-2. Electrochemical Results for C276 in Formate-based Solutions as a Function of Chloride Concentration and Solution Chemistry

Chloride Concentration (ppm)	Chemistry	Average Electrochemical Data					
		CR (mpy)	E_{corr} (V)	i_{pass} (µA/cm²)	E_b (V)	E_{rp} (V)	E_{rp} -E_{corr} (V)
1000	Simple	0.1	-0.122	NA	0.3	0.236	0.358
1000*	Complex	0.5	-0.448	110	0.44	0.245	0.693
1200	Complex	0.1	-0.495	80	0.398	0.260	0.755
800	Complex	0.3	-0.429	175	0.398	0.302	0.735

*Only based on one scan since the duplicate had too much noise to determine values

The CPP scan for the simple chemistry solution was characteristically different than the remaining scans since C276 displayed anodic corrosion without a passivation region (yellow/orange curve in Figure 3-3). The entire scan is also shifted to lower current values indicative of a less corrosive environment for C276. This change in corrosion behavior was not coupled with any change in general corrosion rate as shown by the data in Table 3-2. Although a positive hysteresis was observed, the size of the hysteresis was smaller as indicated by the difference between E_b and E_{rp} (0.065 V versus 0.1-0.2 V for complex chemistry solutions).

The test coupons from the formate-based solutions all showed some degree of change as shown in Figure 3-4. While the rust-colored deposit appears to be corrosion product, the CPP scans and the general CR of less than 0.5 mpy (Table 3-2) indicates another possibility, deposition from a surface reaction. The low CR shows that general corrosion was not aggressive, so corrosion products are not expected. The CPP scans have i_{pass} values on the order of 100 µA/cm^2, larger than i_{pass} for a passive oxide (~1 µA/cm^2). The larger ipass could be caused by a coating deposition from surface reactions. The bullets from the simple chemistry solution (Figure 3-4(A)) showed the least change which agrees with the measured CPP scan at lower current density than the other CPP scans in formate-based solutions. Grinding marks are still readily apparent on the bullet surface, indicating lack of significant corrosion. Test coupons blackened during testing so the potential at which this coating/corrosion products formed could not be determined.

Figure 3-4. Post-test photographs of coupons from formate-based solutions at chloride concentrations of (A) 1000 ppm simple chemistry, (B) 1000 ppm complex chemistry, and (C) 1200 ppm complex chemistry

The bullets were cleaned in 1M nitric acid for 60 seconds with most of the discoloration being removed as shown in Figure 3-5. Grinding marks are still obvious on these surfaces, but also is some degradation. The corrosion is general with some areas of more localized attack as shown especially in Figure 3-4 (B) for the 1000-ppm Cl coupon. These areas were shallow and are not representative of classic pitting. The corrosion may be a result of the destabilized oxide after going through E_b and the large polarization range in the reverse scan back to the E_{corr} value.

Additionally, prior to cleaning a coupon tested in the formate-based solution with 1000 ppm chloride along with a freshly polished coupon were analyzed by x-ray diffraction. The results for the coupon from the 1000 ppm chloride test showed the presence of calcium oxalate and taenite (a Ni-Fe compound) on the surface. The polished coupon did not have the calcium oxalate but iron oxide (FeO) and taenite. While the presence of iron oxide is not surprising, the present of taenite was. This compound may have not been sufficiently removed during the polishing step. Taenite was also the compound found from the potentiostatic testing in formate-based solutions by Fuentes [5].

Figure 3-5. Post-cleaning photographs of coupons from formate-based solutions at chloride concentrations of (A) 1000 ppm simple chemistry, (B) 1000 ppm complex chemistry, and (C) 1200 ppm complex chemistry

Similar to the glycolate-based solutions, the potential difference between E_{corr} and E_{rp} provides a measure of the occurrence of localized corrosion expected in service [16]. For these formate-based solution, $E_{rp} >> E_{corr}$ or E_{rp}-$E_{corr} >>$ 200 mV over the entire range of chloride concentrations tested, so localized corrosion in service is not expected.

The formate-based solutions showed only one region of possible SCC susceptibility, which is that of the positive hysteresis. Again, as in glycolate-based solutions, the CPP scans indicate the electrochemical activity possible for C276, the actual exposure conditions may not drive the sample to these conditions. The coupon immersion test of simulated exposure without accelerating parameters, such as applied potentials, provides a more representative condition for SCC occurrence for the DWPF operating environment.

3.2 Coupon Immersion Testing

Coupon immersion testing is performed to assess a time averaged corrosion behavior for a set of conditions, typically simulating actual exposure environments. For this current testing, the conditions were established in part from the electrochemical results. The electrochemical results clearly indicated that there was no significant difference in the CPP scans and susceptibility to localized corrosion between 800 and 1200 ppm Cl in both formate-based and glycolate-based solutions. Based on these results, the chloride concentrations for the coupon immersion testing were chosen at the current WAC chloride concentration of 800 ppm and the maximum concentration tested, 1200 ppm Cl since no specific localized corrosion was identified on post-test samples.

The coupon immersion test was performed for three months for a total operating time of 2,034 hours. During the operation of the test, vessel temperatures ranged typically between 99 and 101 °C, which was just below a boiling condition for these test solutions. In the initial two weeks, temperatures were more variable as the vessels reached a steady state condition. The maximum measured temperature was 103 °C. Solution loss varied between vessels depending on the effectiveness of the condensers and, in some cases,

the hot plate. Losses were replenished initially with additional solution (up to 500 ml) then switched to distilled water so as not to concentrate the test solutions.

The test coupons were exposed to the solutions on a glass support tree with coupons either completely immersed or attached to a float so that the vapor/liquid interface fell on the coupon. In Figure 3-6 and Figure 3-7, photographs show the coupons on the support after removal from the vessel at the end of the test for the formate-based and glycolate-based solutions, respectively. As can be seen in these photographs, all the coupons had a buildup of sediment from precipitated compounds. These precipitates were not analyzed, although post-test solution analysis of soluble species (see Appendix A) shows that mercury was a component since it was not present in the solution.

Some of the sediment formed an adherent coating on the coupon that required some rubbing to remove as shown by the photographs in Figure 3-7, which show coupons after only rinsing in water. White dotted lines in the figure show the approximate region for the vapor/liquid interface. The actual interface was variable over the three-month test period due to evaporation and slight boiling. The interface is better described as an interfacial region. The rust-colored sentiment may also contain corrosion product. After removing the adherent sentiment, coupons were further cleaned in 1M nitric acid. The interfacial teardrop coupons required up to four minutes soak time and additional brushing. The immersed coupons required 30-60 seconds soak time. The post-cleaning photographs are shown in Figure 3-8. Both before and after cleaning pictures of the front and back for all the coupons are shown in Appendix B.

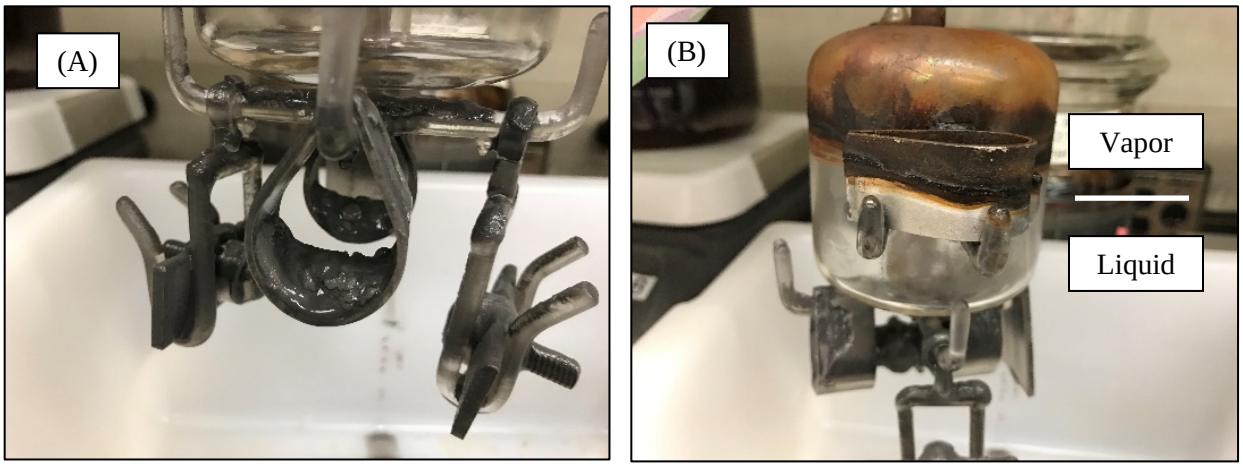

Figure 3-6. Photographs of coupon immersion test coupons immediately after removal from a formate-based solution vessel showing (A) immersed and (B) interfacial coupons

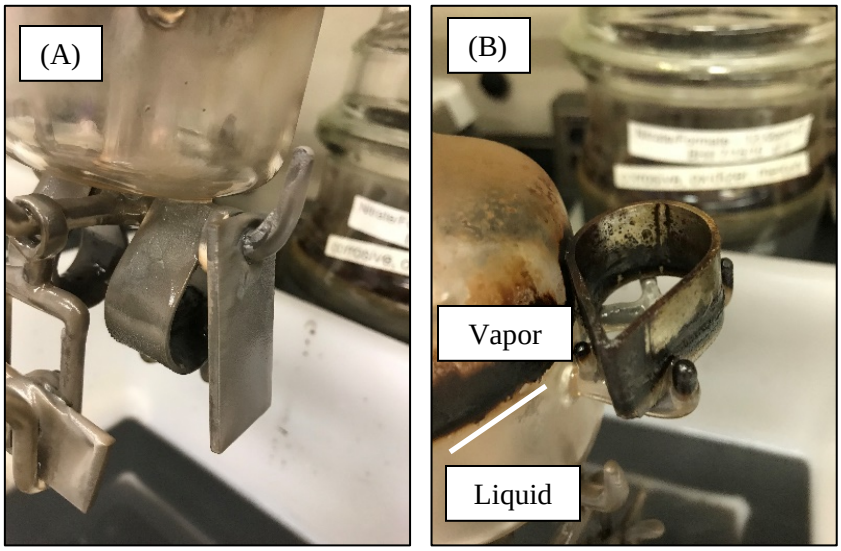

Figure 3-7. Photographs of coupon immersion test coupons immediately after removal from a glycolate-based solution vessel showing (A) immersed and (B) interfacial coupons

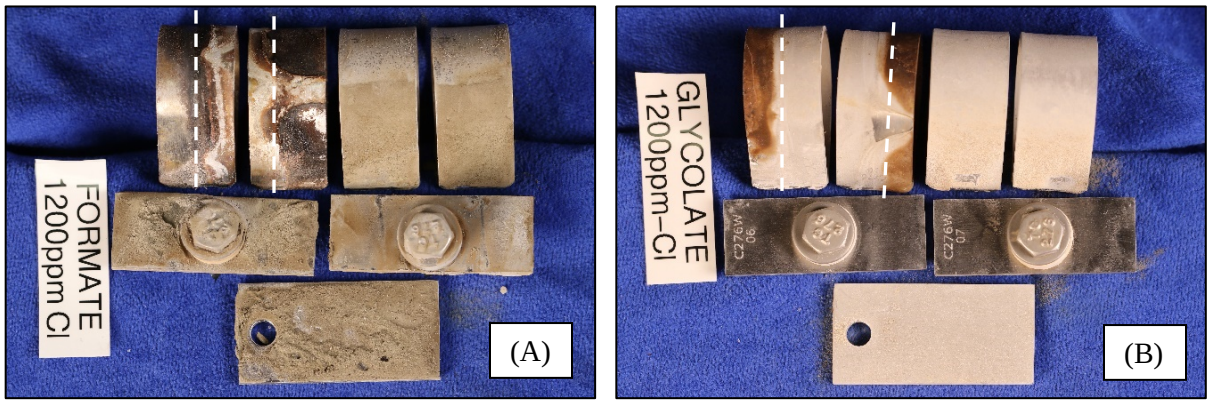

Figure 3-8. Photographs of coupon immersion test coupons at the end of testing after rinsing to remove loose sentiment – (A) formate-based solution and (B) glycolate-based solution (white dotted line indicates vapor/liquid interfacial region with immersed portion of each teardrop facing the other interfacial teardrop)

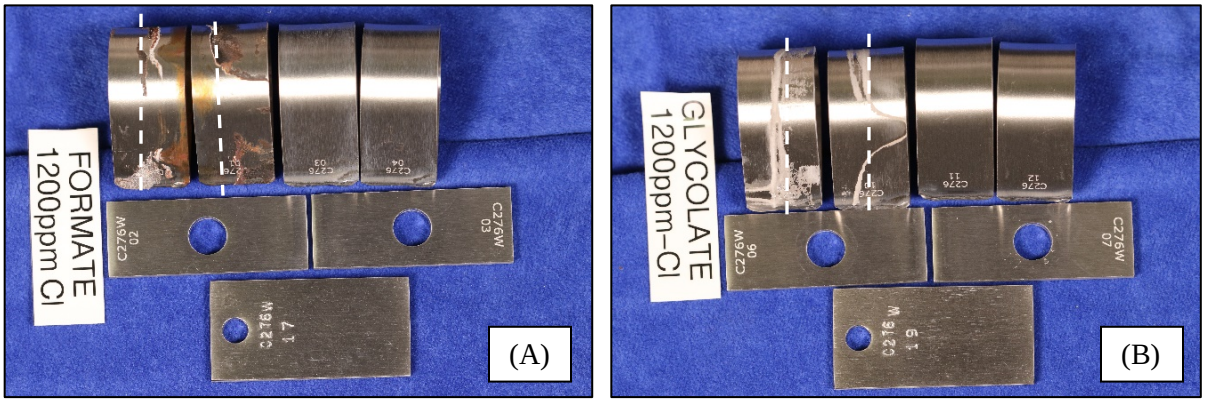

Figure 3-9. Photographs of coupon immersion test coupons at the end of testing after rinsing and nitric acid cleaning – (A) formate-based solution and (B) glycolate-based solution

After cleaning, the coupons were reweighed to determine any weight change. The weight changes for the immersed coupons were small (losses ranged from 0.0001 to 0.0024 g) . Some immersed coupons had residual deposits that were difficult to remove. Extensive effort was not attempted to remove adherent deposits since the coupons would be scarred and have an artificial weight loss. 12 of the 28 coupons had weight gains and residual surface oxides or deposits. Corrosion rates were calculated showing 0.01 mpy or less.

The immersed coupons showed no form of corrosion as can be seen by the coupon photographs taken after the nitric acid cleaning (see Figure 3-8 and Appendix B), including weld attack. In the previous coupon immersion test performed for six months, the weld was highlighted without significant localized corrosion observed [3]. These results demonstrate the corrosion resistance of C276 to these environments including SCC.

The interfacial teardrop coupons differed from immersed coupons in that a greater quantity of tenacious deposits remained after nitric acid cleaning, which resulted in weight gains (see Appendix B for photographs). The teardrops exposed to the formate-based solution had more residual tenacious deposits than teardrops exposed to the glycolate-based solutions, which may be associated with the descaling capability of glycolate [17]. The deposits on the teardrop coupons exposed to the glycolate-based solutions were light in color and had the same appearance as the sediments that were on the coupons during exposure. The deposits on the teardrops exposed to the formate-based solutions were generally black or rust colored similar to steel corrosion products or those observed at the end of electrochemical testing. These deposits may be C276 corrosion products. Post-test solution analyses showed that the glycolate-based solutions had greater soluble quantities of iron and nickel (constituents of C276) than the formate-based solutions. However, the formate-based solutions had more added iron than the glycolate-based solutions. Although the cause of formation for these deposits is unclear, no forms of localized corrosion were identified on these interfacial coupons.

4.0 Discussion

The combined results of the electrochemical and coupon immersion testing have demonstrated the corrosion resistance of C276, including general and localized corrosion, to both glycolate- and formate-based solutions with chloride concentrations up to 1200 ppm at a sulfate concentration of 4200 ppm. The data were consistent with those obtained previously for the determination of WAC limits. In the presence of both reductants, C276 shows passive behavior. In the electrochemical tests, glycolate-based solutions generated lower i_{pass} for C276, but in the formate-based solutions, i_{pass} appeared to be enhanced by a coating deposition. Coupon immersion test results with both reductant-based solutions showed that C276 was not susceptible to SCC or other forms of localized corrosion under simulated conditions at boiling temperatures.

The simple solution tests performed during this testing were used to assess whether earlier data from the 1980s material testing performed initially for DWPF give similar results to the current approach of using more complex solutions. The exact solution chemistry that was used in this earlier testing is unclear as based on a review of available literature. In a report by Carlson which presented test data, the solutions annotated for these results had only two to five components [10]. Whether the solutions contained only these components or whether these were the only components that were changed is not provided in the Carlson report. Corbett et al. reported that the solutions were “formulated based on concentration of major chemical components” but provided solution chemistry that only contained chloride, fluoride, sulfate and mercury with the pH[2] adjusted by formic or sulfuric acid [18]. If only these species were present, the solution would be aggressive and provide a conservative measurement for material selection. In another reporting of the testing by Bickford and Corbett, the information provided stated, “Test solutions were formulated based upon major chemical components, acidic species, and ionized transition metals that are

[2] Reported pH values used for testing were 4 and 6.

known to enhance general or localized attack (e.g., cupric and ferric ions).", although the same solution chemistry was provided as given by Corbett et al. [18, 19].

Since the information on previous solution chemistry was unclear and nitrates are present in incoming waste at significant concentrations, this species was included along with other known aggressive species – chloride, sulfate and mercury. Fluoride at the concentrations processed in the DWPF were not shown to play a factor in material corrosion.

As shown in the results, differences between the simple and complex chemistry test solutions was a function of the reductant. For glycolate-based solutions, the passivation of the surface (i.e., presence of passivation peak) and the breakdown of that surface (i.e., positive hysteresis) were similar for the two chemistry formulations. The general corrosion rate and i_{pass} were slightly higher for the simple chemistry. For the formate-based solutions, C276 exhibited anodic corrosion with low corrosion rates in the simple chemistry but passive behavior in the complex chemistry. In both solutions, a positive hysteresis was observed. For both these reductants, the difference in results from solutions with simple and complex chemistry were small and did not alter the overall conclusion on the influence of the reductant on the material.

5.0 Conclusions

During the test program to assess the influence of glycolic acid/glycolate on the MoCs within waste management facilities, SCC initially had not been a major concern nor specifically tested. SCC resistance of the MoCs within the DWPF is specifically stated in the DWPF SIP. Some waste environments are not conducive to the occurrence of SCC and in some cases, such as the Tank Farm, a corrosion control program is in place to minimize the occurrence of SCC. Solution chemistry within the CPC of the DWPF was found to cause some localized corrosion for C276. SCC, however, was never fully tested to assess the influence of occurrence under these boiling conditions, which increases the likelihood of SCC. Electrochemical tests along with stressed coupon immersion tests were conducted specifically to demonstrate that SCC was not likely for CPC vessels.

The results from both the electrochemical and coupon immersion tests in formate-based and glycolate-based solutions with chlorides concentrations between 800 and 1200 ppm demonstrated that there were no active forms of localized corrosion. The CPP scans in these solutions had passive regions with some degree of positive hysteresis which indicate a possibility for the occurrence of localized corrosion. The positive hysteresis occurred at potentials greater than 200 mV more electropositive that E_{corr} indicating that, at least, crevice corrosion should not occur in service. The three-month coupon immersion tests, however, demonstrated that no form of localized corrosion (SCC, crevice corrosion and pitting) occurred under simulated operating conditions. The coupon immersion test also showed that deposits are likely to form on C276 during service, especially near the vapor/liquid interface.

The testing also showed that some differences occur with using simple DWPF simulants as opposed to the more complex solution chemistry used in this testing. The testing was performed to establish a comparison point between older corrosion data obtained with simple solution chemistry and the newer data. For glycolate-based solutions, which were not tested prior to this study, did not show a significant difference. For formate-based solutions, the difference was more significant with a change in operable corrosion mechanisms (i.e., anodic corrosion for a simple chemistry versus passivity for a complex chemistry). However, the lack of susceptibility to localized corrosion was found to be the same.

6.0 References

1 T. L. Fellinger, "Influence of Nitric-Glycolic Acid Flowsheet – Material Evaluation for DWPF and Downstream Tank Farm Processes," HLW-DWPF-TTR-2013-0004, Revision 0, 2012

2 J. I. Mickalonis et al, "Corrosion Influence of Alternate Reductant on DWPF and Downstream Facilities," SRNL-STI-2014-00281, Revision 0, December 2014

3 J. I. Mickalonis, "Impact of Glycolate Anion on Aqueous Corrosion in DWPF and Downstream Facilities," SRNL-STI-2015-00482, Revision 3, 2019

4 J. W. Ray, "Waste Acceptance Criteria for Raw Salt Solution, Sludge, and SWPF Salt Stream Transfers to DWPF," X-SD-S-00001, Revision 27, 2018

5. R. E. Fuentes, "Impact of Permanganate Oxidation of Glycolate on corrosion of the Defense Waste Processing Facility (DWPF) Recycle Collection Tank (RCT), Transfer-line and Tank 22 Materials of Construction (MoC), SRNL-STI-2019-00742, Revision 0, 2020

6. M. S. Williams et al, "Corrosion Testing of Monofrax™ K-3 Refractory in Defense Waste Processing Facility (DWPF) Alternate Reductant Feeds," SRNL-STI-2016-00030, 2016

7 W. L. Daugherty, "Evaluation of Potential for Materials Degradation of DWPF Safety Class and Safety Significant Components," WSRC-TR-95-0385, Revision 0, 1995

8 J. I. Mickalonis, "Task Technical and Quality Assurance Plan for Material Evaluation for DWPF Nitric-Glycolic Acid Flowsheet," SRNL-RP-2012-00834, Revision 3, 2017

9 J. I. Mickalonis and R. E. Fuentes, "Run Plan for Stress Corrosion Cracking Determination in Support of DWPF Alternate Reductant," SRNL-L5400-2019-00005, Revision 0, 2019

10 M. K. Carlson, "DWPF Corrosion Report Database," OPS-WMQ-890082, 1989

11 ASTM G5 – 14, "Standard Reference Test Method for Making Potentiodynamic Anodic Polarization Measurements," ASTM International, West Conshohocken, PA 2018

12 ASTM G59 – 97 (Reapproved 2014), "Standard Test Method for Conducting Potentiodynamic Polarization Resistance Measurements," ASTM International, West Conshohocken, PA 2018

13 ASTM G61 – 86 (Reapproved 2014), "Standard Test for Conducting Cyclic Potentiodynamic Polarization Measurements for Localized Corrosion Susceptibility of Iron-, Nickel-, or Cobalt-Based Alloys" ASTM International, West Conshohocken, PA 2018

14 ASTM G102 – 89 (Reapproved 2015), "Standard Practice for Calculation of Corrosion Rates and Related Information from Electrochemical Measurements," ASTM International, West Conshohocken, PA 2018

15 ASTM G31 – 12a, "Standard Guide for Laboratory Immersion Corrosion Testing of Metals," ASTM International, West Conshohocken, PA 2018

16 D.C. Silverman, "Practical Corrosion Prediction Using Electrochemical Techniques," R. W. Revie (ed), Uhlig's Corrosion Handbook, 2nd Ed, J. Wiley & Sons, 2000

17 J. I. Mickalonis and T. E. Skidmore, “Material Compatibility Evaluation for DWPF Nitric-Glycolic Acid – Literature Review,” SRNL-STI-2013-00281, Revision 0, 2013

18 R. A. Corbett, D. F. Bickford, and W. S. Morrison, “Corrosion Evaluation of Alloys for Nuclear Waste Processing,” Corrosion86, Paper No. 254, 1986

19 D. F. Bickford and R. A. Corbett, “Material Selection for Defense Waste Processing Facility,” DP-MS-84-128, 1984

Appendix A. Analyzed Compositions of SCC Test Solutions Post-Testing

Post-test analyses was performed on the coupon immersion test solutions. These analyses show the soluble elements at the end of the test.

Constituent	Units	Formate-based		Glycolate-based	
		Cl=800 ppm	Cl=1200 ppm	Cl=800 ppm	Cl=1200 ppm
Hg	mg/L	0.0109	0.0103	0.165	0.248
F	µg/mL	<10	<10	<10	<10
CO_2H	µg/mL	77800	61800	<100	<100
Cl	µg/mL	997	1240	822	1360
NO_2	µg/mL	15	21.9	<10	<10
NO_3	µg/mL	61200	49200	65600	70100
PO_4	µg/mL	<10	<10	<10	<10
SO_4	µg/mL	5570	4400	4560	4850
C_2O_2	µg/mL	2020	1590	3970	4300
Br	µg/mL	<50	<50	<50	<50
Glycolate	mg/L	<500	<500	52900	52300
Ag	mg/L	<0.327	<0.327	<0.327	<0.327
Al	mg/L	<0.566	<0.566	253	272
B	mg/L	14	12.6	2.73	2.79
Ba	mg/L	<0.417	<0.417	<0.417	<0.417
Be	mg/L	<0.031	<0.031	<0.0313	<0.031
Ca	mg/L	5.51	4.92	43	44.1
Cd	mg/L	<0.074	<0.074	<0.0741	<0.074
Ce	mg/L	<1.62	<1.62	<1.62	<1.62
Co	mg/L	<0.813	<0.813	<0.813	<0.813
Cr	mg/L	<0.556	<0.556	<0.556	<0.556
Cu	mg/L	<0.556	<0.556	<0.556	<0.556
Fe	mg/L	<0.496	<0.496	41.3	45.1
K	mg/L	371	381	363	380
La	mg/L	<1.06	<1.06	<1.06	<1.06
Li	mg/L	<0.992	<0.992	<0.992	<0.992
Mg	mg/L	206	219	219	231
Mn	mg/L	707	913	2720	2910
Mo	mg/L	<0.864	<0.864	<0.864	<0.864
Na	mg/L	50600	55400	38800	41900
Ni	mg/L	2.6	3.76	55.3	65.8
P	mg/L	<3.08	<3.08	<3.08	<3.08
Pb	mg/L	<0.793	<0.793	<0.793	<0.793
S	mg/L	1590	1650	1560	1620
Sb	mg/L	<2.66	<2.66	<2.66	<2.66
Si	mg/L	<9.39	14.3	16	16.9
Sn	mg/L	<7.56	<7.56	<7.56	<7.56
Sr	mg/L	0.035	0.034	0.039	0.084
Ti	mg/L	<0.068	<0.068	<0.068	<0.068
V	mg/L	<0.076	<0.076	<0.076	<0.076
Zn	mg/L	<0.394	<0.394	0.257	0.485
Zr	mg/L	<0.087	<0.087	1.45	1.93

Appendix B. Post-test Photographs of Immersion Test Coupons*

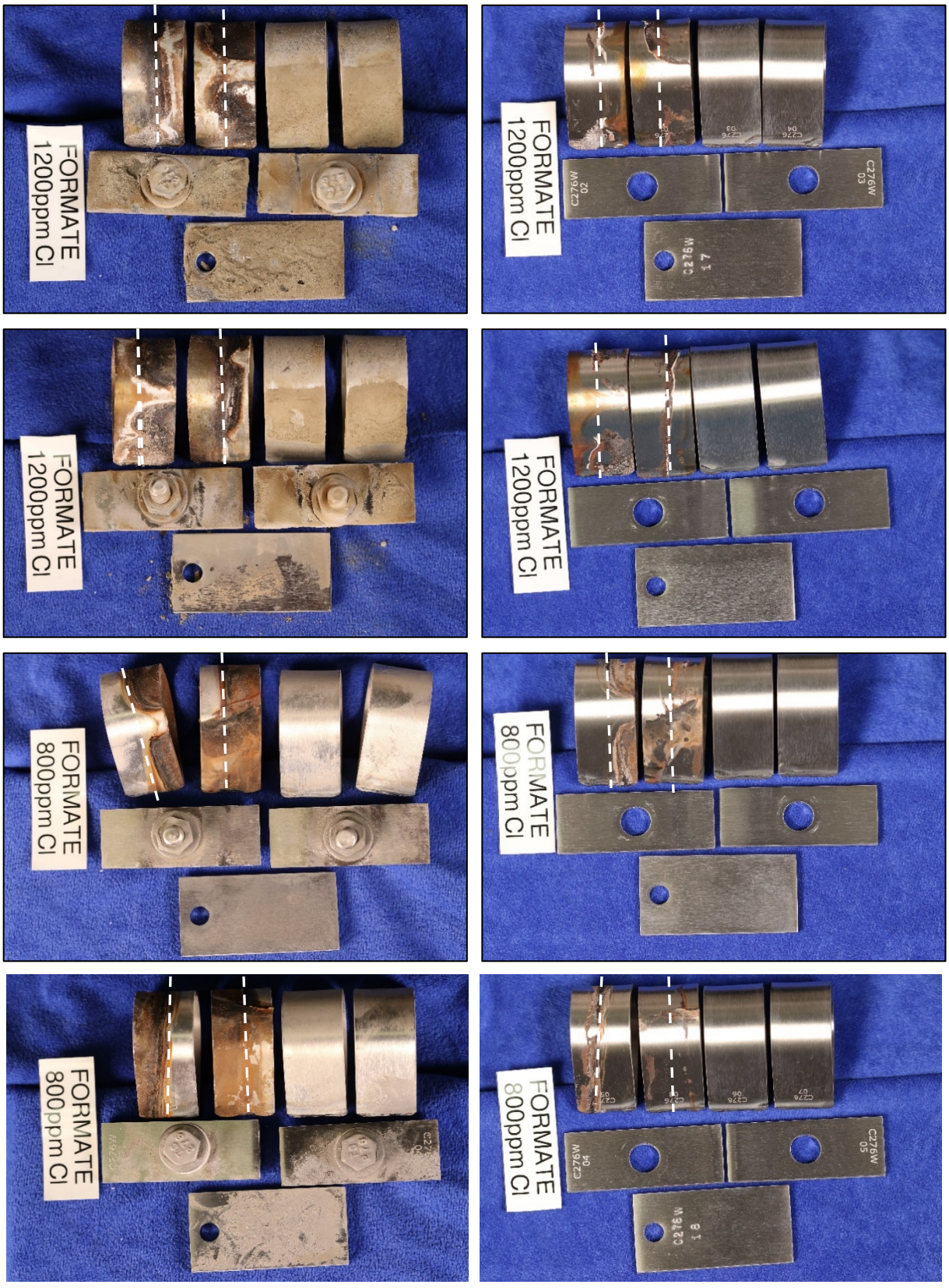

*White dotted lines indicate approximate location of vapor/liquid interface.

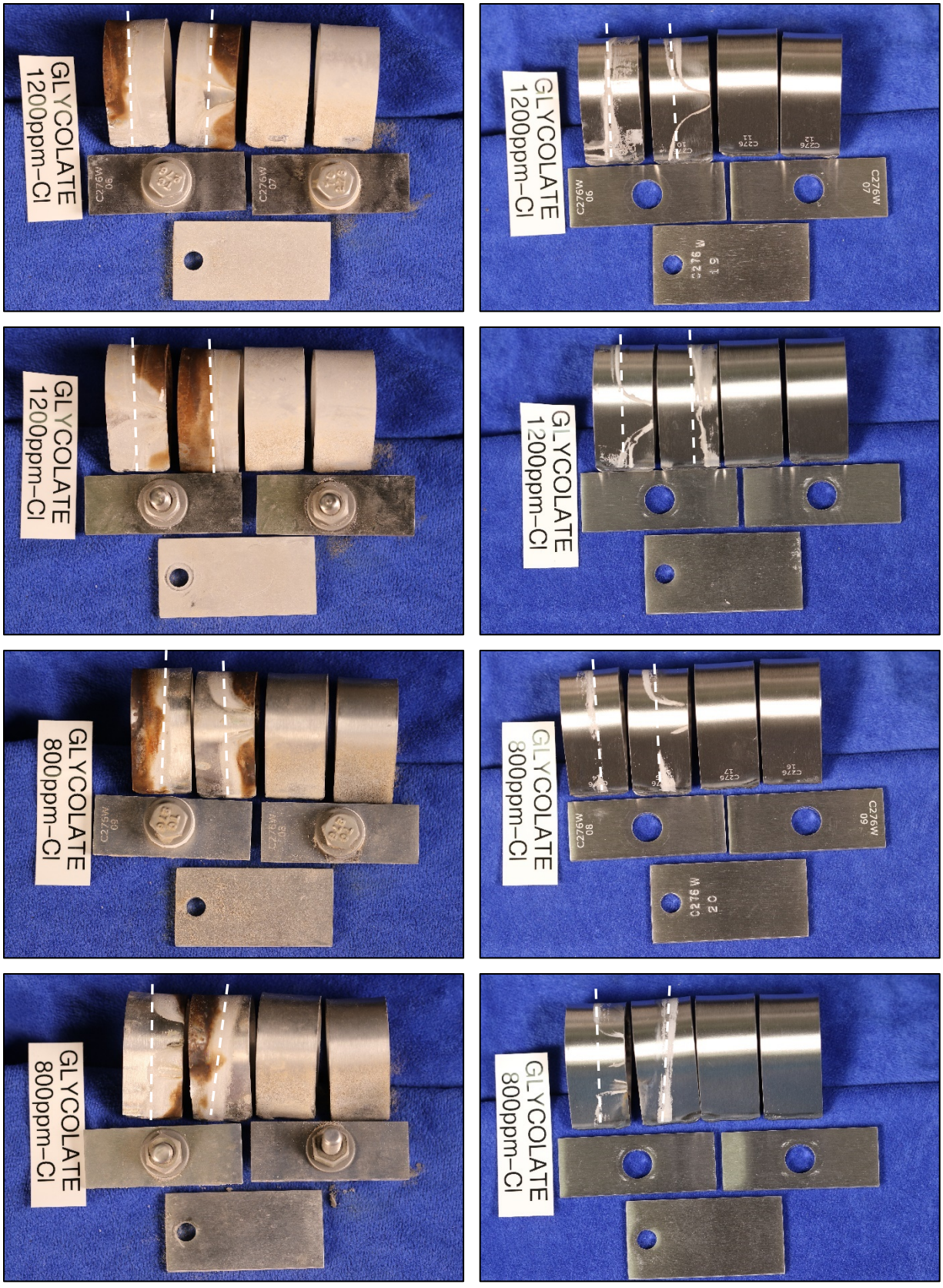
GLYCOLATE
1200ppm–Cl
GLYCOLATE
1200ppm–Cl
GLYCOLATE
800ppm–Cl
GLYCOLATE
800ppm–Cl
GLYCOLATE
1200ppm–Cl
GLYCOLATE
1200ppm–Cl
GLYCOLATE
800ppm–Cl
GLYCOLATE
800ppm–Cl

Distribution:

alex.cozzi@srnl.doe.gov
david.crowley@srnl.doe.gov
a.fellinger@srnl.doe.gov
samuel.fink@srnl.doe.gov
Brenda.Garcia-Diaz@srnl.doe.gov
connie.herman@srnl.doe.gov
dennis.jackson@srnl.doe.gov
Joseph.Manna@srnl.doe.gov
daniel.mccabe@srnl.doe.gov
Gregg.Morgan@srnl.doe.gov
frank.pennebaker@srnl.doe.gov
Amy.Ramsey@srnl.doe.gov
William.Ramsey@SRNL.DOE.gov
eric.skidmore@srnl.doe.gov
michael.stone@srnl.doe.gov
Boyd.Wiedenman@srnl.doe.gov
chris.martino@srnl.doe.gov
thomas.colleran@srs.gov
richard.edwards@srs.gov
bill.holtzscheiter@srs.gov
spencer.isom@srs.gov
vijay.jain@srs.gov
MARIA.RIOS-ARMSTRONG@SRS.GOV
robert.hoeppel@srs.gov
jeff.ray@srs.gov
kevin.brotherton@srs.gov
celia.aponte@srs.gov
timothy.baughman@srs.gov
earl.brass@srs.gov
thomas.huff@srs.gov
ryan.mcnew@srs.gov
phillip.norris@srs.gov
christine.ridgeway@srs.gov
azadeh.samadi-dezfouli@srs.gov
christie.sudduth@srs.gov
arthur.wiggins@srs.gov
terri.fellinger@srs.gov
jeffrey.gillam@srs.gov
barbara.hamm@srs.gov
hasmukh.shah@srs.gov
aaron.staub@srs.gov
james.folk@srs.gov
roberto.gonzalez@srs.gov
patricia.suggs@srs.gov
roderick.fuentes@srnl.doe.gov